International Journal of Pure and Applied Chemistry, Volume 2, Issue 1, 2024
Article DOI: https://doi.org/10.37284/ijpac.2.1.2242

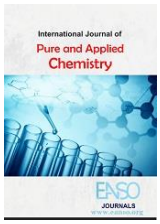

International Journal of Pure and Applied Chemistry
ijpac.eanso.org
Volume 2, Issue1, 2024
Print ISSN: 2790-9565 | Online ISSN: 2790-9573
Title DOI: https://doi.org/10.37284/2790-9573

EAST AFRICAN NATURE & SCIENCE ORGANIZATION

Original Article

Chitosan Coupled Silver Nanoparticles Electrocatalyst Synthesis and Characterization

Martin Osemba[1], Prof. Mary Muriuki-Hutchins, PhD[2], Dr. Samuel Karenga, PhD[1] & Dr. Godffrey Keru, PhD[3]*

[1] Mount Kenya University, P. O. Box 342-01000, Thika, Kenya.
[2] Harris–Stowe State University, St. Louis, MO 63103, USA.
[3] Whitworth University, Spokane, WA 99251, USA.
[*] Author for Correspondence Email: osembamartin@gmail.com

Article DOI: https://doi.org/10.37284/ijpac.2.1.2242

Date Published:

25 September 2024

Keywords:

Silver Nanoparticles, Chitosan, Coupling, Synthesis, Characterization.

ABSTRACT

This study sought to find a suitable technique for synthesizing and characterizing silver nanoparticles due to its applications in various fields such as nanotechnology and medical. The synthesized silver nanoparticles were characterized using SEM microscopy, FT-IR and UV-Vis spectroscopy. The maximum absorbance from the UV-Vis spectrophotometer showed the formation of silver nanoparticles with λ max of 418 nm. The FTIR analysis envisaged a strong symmetrical stretching at 1400 cm-1 to 1200 cm-1 with the major peaks recorded at 1390 cm-1 and 1380 cm-1, indicating the presence of nitro components in the sample. The signal at 1658 cm−1 corresponded to the amide (C=O) bonds stretching vibrations, at 1089 cm−1 C-O-C bonds and at 564 cm−1 plane with bends NH, plane-out and bends C−O. C-H stretching vibrational signal was noted at 2927 cm−1, and a broader band at 3426 cm−1 with an overlap between the O−H stretching vibration and N−H stretching vibration of the oligosaccharide applied in the capping. The concentration of chitosan on transmittance was done using 0.5%, 1.0%, 1.5% and 2.0% solutions with the results from FT-IR showing elaborate intensity at 2.0 % chitosan capping and the least at 0.5 %. Scanning microscope validated characterized silver nanoparticles morphology at 500nm. The results obtained from SEM depicted a size range of 100 nm with resolutions between 0.5 to 4 nm.

APA CITATION

Osemba, M., Muriuki-Hutchins, M, Karenga, S. & Keru, G. (2024). Chitosan Coupled Silver Nanoparticles Electrocatalyst Synthesis and Characterization *International Journal of Pure and Applied Chemistry*, *2*(1), 1-12. https://doi.org/10.37284/ijpac.2.1.2242.

Article DOI: https://doi.org/10.37284/ijpac.2.1.2242

CHICAGO CITATION

Osemba, Martin Osemba, Mary Muriuki-Hutchins, Samuel Karenga and Godffrey Keru. 2024. "Chitosan Coupled Silver Nanoparticles Electrocatalyst Synthesis and Characterization". *International Journal of Pure and Applied Chemistry* 2 (1), 1-12. https://doi.org/10.37284/ijpac.2.1.2242.

HARVARD CITATION

Osemba, M., Muriuki-Hutchins, M, Karenga, S. & Keru, G. (2024) "Chitosan Coupled Silver Nanoparticles Electrocatalyst Synthesis and Characterization", *International Journal of Pure and Applied Chemistry*, 2(1), pp. 1-12. doi: 10.37284/ijpac.2.1.2242.

IEEE CITATION

M. Osemba, M. Muriuki-Hutchins, S. Karenga & G. Keru. "Chitosan Coupled Silver Nanoparticles Electrocatalyst Synthesis and Characterization", IJPAC, vol. 1, no. 2, pp. 1-12, Sep. 2024.

MLA CITATION

Osemba, Martin, Mary Muriuki-Hutchins, Samuel Karenga & Godffrey Keru. "Chitosan Coupled Silver Nanoparticles Electrocatalyst Synthesis and Characterization". *International Journal of Pure and Applied Chemistry*, Vol. 2, no. 1, Sep. 2024, pp. 1-12, doi:10.37284/ijpac.2.1.2242.

INTRODUCTION

Silver nanoparticles are used in variety of fields, including air filtration and quality management, bio-sensing, imaging, and drug delivery (Kaushal et al., 2023). Silver nanoparticles generated biologically have various potential uses, such as antimicrobials, optical receptors, catalysts in chemical detection reactions, bio labels, and coatings for solar power absorption (Shehabeldine et al., 2022). Despite their cytotoxicity, silver nanoparticles find widespread use in sectors as diverse as bimolecular analysis of high-sensitivity, diagnostics, antibacterial and therapies, catalysis, and micro-electronics chips (Algethami et al., 2022). Applications in medicine, such as wound dressings, contraceptive devices, surgical equipment, and bone prosthesis, have also been proposed (Husain et al., 2023). Other possible uses include in diagnosis and bio-imaging, optical densities imaging, and bio-implants e.g., heart valves (Arshad et al., 2024). Several large consumer goods companies are currently making domestic products that make use of silver nanoparticles' antibacterial qualities (Fernandez et al., 2021). Silver nanoparticles are utilized in a variety home appliance, including refrigerators, air conditioners, and washers (Naganthran et al., 2022). Nanoparticles have unique physicochemical qualities that make them ideal candidates for various applications (Osemba, 2019). These characteristics include a large surface area to volume ratio, mechanical strength, optical property, and their overall chemistry (Nie et al., 2023). To prevent the spread of disease, silver nanoparticles are incorporated in an inorganic antibacterial agent (Bruna et al., 2021). It has been hypothesized that the ions of silver have both a bacteriostatic (growth inhibition) and bactericidal (antibacterial) effect (Dawadi et al., 2021), hence the term "oligodynamic" to characterize silver. Silver nanoparticles have various biological uses for instance antibacterial medicines are resistant to bacterial infection, enable wound healing and possess anti-inflammatory effects (Kowalczyk et al., 2021). They are also toxic towards microorganisms, by showing potent biocidal effect on different types of bacteria (Choudhary et al., 2022), although they are rather non-lethal to mammalian cells. Thus, dental resin composites, bone cement, natural process fibers, and coatings for medical equipment all include silver ions, an antibacterial component (Azevedo et al., 2024). Electronic effects coming from the localized electronic structure on the surface of nanoparticles are responsible for their bactericidal action (Ahmed et al., 2024). These modifications are thought to increase silver nanoparticle surface reactivity (Arshad et al., 2024). The ionic form of silver has been shown to inhibit vital enzymes by forming strong interactions with their thiol groups (Younis,

Article DOI: https://doi.org/10.37284/ijpac.2.1.2242

2024). It is also hypothesized that after interacting with silver ions, bacteria's DNA loses its capacity to replicate (Kar et al., 2024). By attacking the bacterial membrane, silver nanoparticles disrupt the cell wall potential and accelerate intracellular (ATP) depletion, ultimately killing the bacteria (Behera et al., 2024). In light of these numerous applications of silver nanoparticles, saw the quest for its synthesis and characterization through coupling with the chitosan (Osemba et al., 2024).

EXPERIMENTAL

Preparation of chitosan-coupled silver nanoparticles

Stable silver nanoparticles were synthesized using chitosan acting as both reducing and stabilizing agent without using any toxic chemicals. This reaction was carried out in an autoclave at a pressure of 15 psi and 120.0 ^{o}C temperature by varying the time. Analytical grade silver nitrate was purchased from the commercial suppliers (Sigma-Aldrich). 0.200g of the chitosan was dissolved in 1 % acetic acid solution followed by magnetic stirring for 30 minutes. The mixture solution was then filtered to obtain clear solution of chitosan- acetic acid mixture. Then 3.00 mL of 0.1M solution of freshly prepared of silver nitrate was added to the mixture. 100 µL of 1.0 M sodium hydroxide was also added and then the mixture was stirred for 10 hours using a magnetic stirrer at 90.0°C. Centrifugation was then carried out at 3500 rpm for 30 minutes to isolate the silver nanoparticles formed

Characterization

Both spectroscopic and microscopic techniques were applied in this study for the characterization of the synthesized samples. They include the following: - Furiour transform infrared (FT-IR), ultraviolet (UV-Vis) and scanning electron microscope (SEM). UV-visible spectral analysis of the silver nanoparticles was accomplished using UV-Vis spectrophotometer (Shimadzu UV 2500 Japan model) for determination of maximum absorption spectrum, which should occur between 410- 420 nm of wavelength. Furiour transform infrared (FT-IR) spectroscopy analysis for functional group determination using IR spectrophotometer (Shimadzu model 8400). Scanning electron microscopy was then used for the visualization of the morphology of the nanoparticles using (JEOL 2010).

FT-IR analysis

Furiour transform infrared spectroscopy was applied in the analysis of the chitosan, silver nano-composite film electrodes. The spectra were obtained over 16 scans covering the 4000-400 cm^{-1} wave-number range at 4 cm^{-1} resolution and at 25.0 using a Thermo Scientific Nicolet iS10 FTIR spectrometer.

UV-Vis spectroscopic analysis

The study of the optical characterization of the synthesized metallic nanoparticles was observed during this research work with the assistance of a double beam 3000+ LABINDIA, UV-Vis spectrophotometer and a cell of 1.0 cm path length within the spectral range 200-800 nm. Effect of temperature on kinetic study of reaction was studied by a Peltier accessory (temperature-Controller) model PTC-2 is linked with the UV-Visible spectrophotometer. Two lamp combinations are utilized in double beam spectrophotometer one is deuterium lamp used for UV part and second is tungsten lamp used for the visible part. Sample cell is formed by Quartz and lightweight beam travels a distance of 1 cm through the sample. For obtained UV spectra of our sample first done baseline by reference in order that other reagent peaks were nullified, then obtain the spectra

Scanning Electron Microscopy characterization of silver nanoparticles

Scanning microscope was used to validate the characterization of silver nanoparticles by giving nutshell description by providing the necessary

Article DOI: https://doi.org/10.37284/ijpac.2.1.2242

information concerning the morphology of these silver nanoparticles. These images were taken at 500nm. The results of the nanoparticles as shown in the plates 2 *a, b, c* below show the results obtained from the scanning electron microscope (SEM) depicted a picture of these nano-particle exhibiting size range of 100 nm which are in agreement with the earlier findings on the right sizes at different resolutions between 0.5 to 4 nm. Size of synthesized nanoparticles was more than the size of nanoparticles which should be between 1-100nm.

RESULTS AND ANALYSIS

Results of the characterization of silver nanoparticles using FT-IR Spectroscopy

The characterization of silver nanoparticles was achieved using FT-IR (Frontier Spectrometer, Perkins Elmer, USA). These silver nanoparticles were dried at a temperature of 80^{o}C, then ground with anhydrous KBr for the formation of pellets for easier characterization in the Furiour transform infrared spectroscopy within the absorption frequency range of between 4000 cm^{-1} to 400 cm^{-1}. FT-IR analysis provided spectra with different peaks as shown in figure 1 below. These vibration signals were useful in the identification of the functional groups found in the silver nanoparticles samples applied in the research study.

Figure 1: Showing FT-IR spectrum of silver nanoparticles capped chitosan

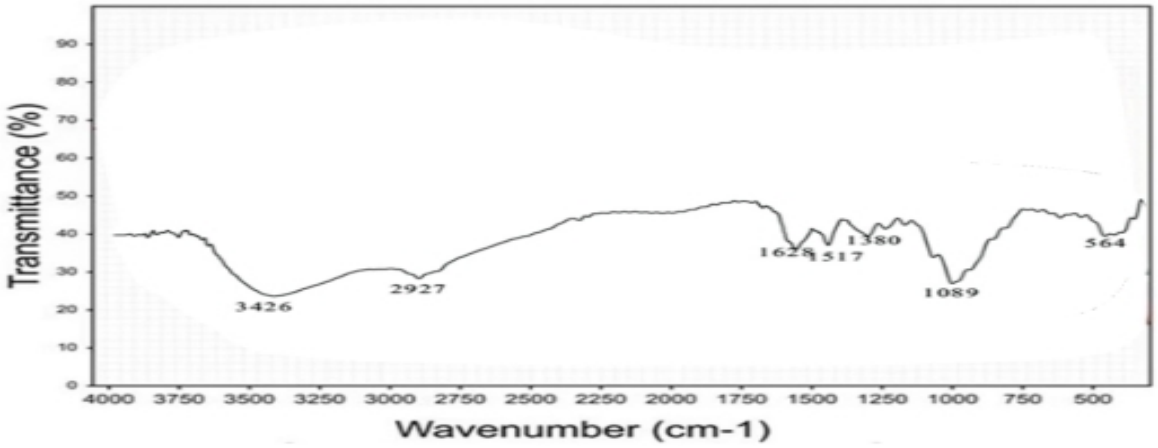

Figure 1 shows an FT-IR graph whose x-axis represents the wave-numbers (cm^{-1}) of infrared spectra whereas, y-axis represents the transmittance (%) of the sample applied. The absorption bands, correspond to different vibrations of atoms in the sample applied when it was exposed to the infrared region of the electromagnetic spectrum. The results obtained envisaged a strong symmetrical stretching at the range of 1400 cm^{-1} to 1200 cm^{-1} with the major peaks recorded at 1390 cm^{-1} and 1380 cm^{-1}, indicating the presence of nitro component in the sample. The following signals presented in the spectrum in figure 1 above were obtained from the FT-IR analysis. The signal at 1658 cm^{-1} corresponded to the amide (C=O) bonds stretching vibrations. The signal shown at 1089 cm^{-1} represents secondary alcohol (C-O-C) bonds whereas, the peaks show sharpness at 564 cm^{-1} plane with bends NH, plane-out and bends C−O. C-H stretching vibrational signal was noted at 2927 cm^{-1}, a broader band at 3426cm^{-1} for an overlap between the O−H stretching vibration and the N−H stretching vibration of the oligosaccharide applied in the capping. The obtained results are in

Article DOI: https://doi.org/10.37284/ijpac.2.1.2242

agreement with the findings on the functional groups in silver nanoparticles formed in the bio-reduction techniques in which, chitosan macro-molecules are found to be acting not only as reducing but also capping agent. It is important to note that the intensity of the O−H and N−H stretching bands emanated from the hydroxyl and amino groups thus shifting to 3426 cm^{-1} from 3434 cm^{-1} wave number of the chitosan in the FT-IR spectrum as shown in figure 4.0, implying that chelation of silver with both O−H and N−H groups of chitosan actually took place.

Results of different levels of chitosan applied in the synthesis of silver nanoparticles

The impact of concentration of chitosan on transmittance during the synthesis of silver nanoparticles was done using 0.5%, 1.0%, 1.5% and 2.0% solutions. The results obtained using FT-IR. (Frontier Spectrometer, Perkins Elmer, USA), were presented in figures 2 (a,b,c and d) below. Analysis was carried out in the wavelength range of 450 - 4000 cm^{-1} at a resolution of 4 cm^{-1}).

Figure 2(a): Showing FT-IR spectrum of silver nanoparticles capped with 0.5% chitosan

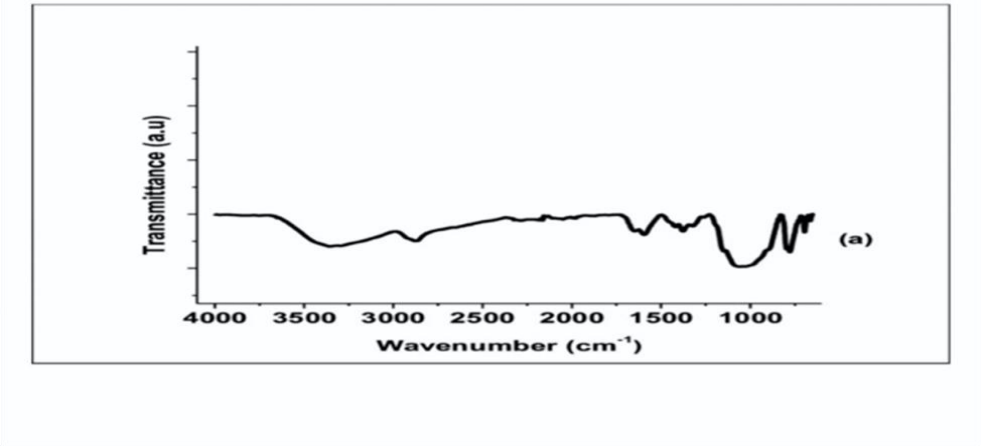

Figure 2 (b): Showing FT-IR spectrum of silver nanoparticles capped with 1.0 % chitosan

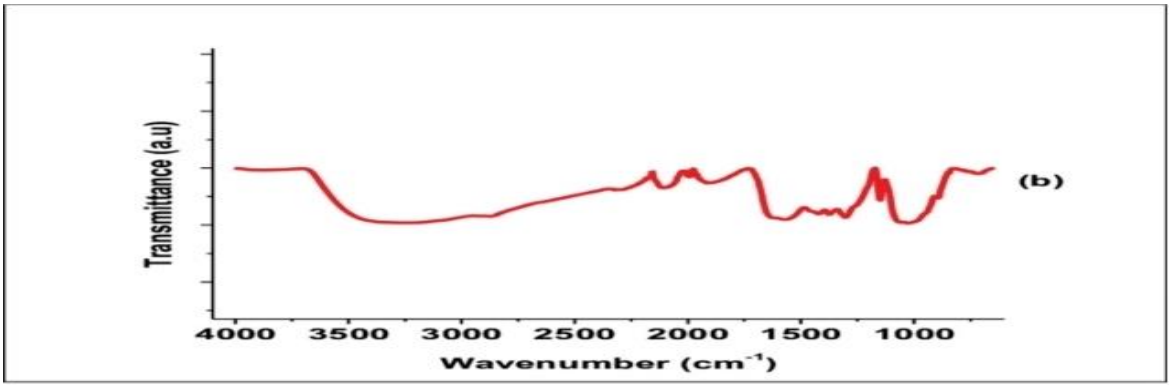

Article DOI: https://doi.org/10.37284/ijpac.2.1.2242

Figure 2 (c): Showing FT-IR spectrum of silver nanoparticles capped with 1.5 % chitosan

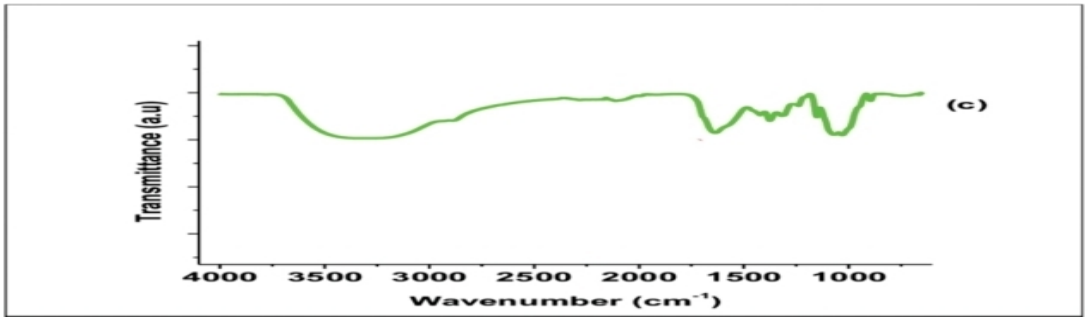

Figure 2 (d): Showing FT-IR spectrum of silver nanoparticles capped with 2.0 % chitosan

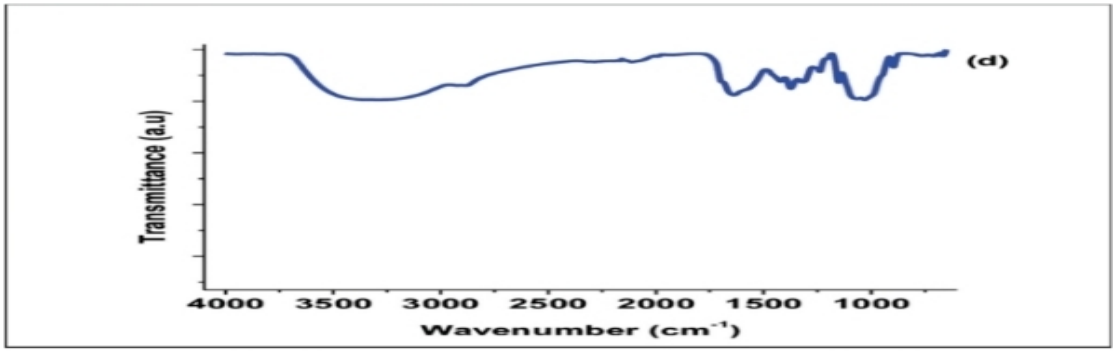

The Figures 2(*a, b, c,* and *d)* above represent the data obtained from the FT-IR and interpreted using the spectral lines of infrared by comparing the correlation of bands in the absorbance spectrum to that of the silver nanoparticles samples capped with 0.5, 1.0, 1.5 and 2.0 % chitosan respectively and applied during the experiment. It was also noted that intensity of transmittance was much elaborate at 2.0 % chitosan capping compared to the least at 0.5 %. FT-IR spectroscopy was able to effectively determine the formation of silver nanoparticles. During this characterization it was confirmed that the breadth and intensities of peaks taken from infrared spectrum, explicitly depended on the sizes of silver nanoparticles under scrutiny.

Results of the characterization of synthesized silver nanoparticles using UV-Vis

The characterization of the synthesized silver nanoparticles was performed using a UV-Vis spectrophotometer (double beam 3000+ LABINDIA) and a cell of 1.0 cm path length within the wavelength range of 200-800 nm. Two lamp combinations are utilized in double beam spectrophotometer one is deuterium lamp used for UV part and second is tungsten lamp used for the visible part. Sample cell was formed by Quartz and lightweight beam travels a distance of 1 cm through the sample. For obtained UV spectra of our sample in figures 3 below, first and foremost, baseline by reference was done in order to nullify peaks for any other reagent present, then obtain the spectra for the sample of the silver nanoparticles. Therefore, the figures 3 below represents synthesized silver nanoparticles scanned between 400 nm to 500 nm wavelength using the UV-Vis spectrophotometer. The maximum absorbance from the UV-Vis spectrophotometer showed the formation of silver nanoparticles with λmax of 418 ± 2 nm. The synthesized silver nanoparticles were analyzed using UV-Vis spectroscopy, the analysis exhibited spectral line readings at different time intervals commencing with the initiation stage of the reaction. Ultraviolet-visible spectroscopy allows the resonance of the oscillation by conducting electrons within the interfaced band occurring at the negative and positive permittance in the materials

Article DOI: https://doi.org/10.37284/ijpac.2.1.2242

undergoing stimulation through incidence of light. Surface plasmon resonance, highly dependents on the sizes of the silver nanoparticles present. The study showed that the shape of these nanoparticles played a very crucial role in actualizing the surface plasmon position of the band formed. Technically, the applications of silver nanoparticles and the control in process utilizes the in-situ model of concentration determination, distribution in size and the dielectric aspects. The absorption spectral lines of silver nanoparticles are optically over shadowed by SPR, this is in line with other finding in the earlier studies. Therefore, longer wavelengths were determined in the cases where particle sizes had shown increase. This study confirmed that position and shape in the absorbance within the surface plasmon resonance of silver nanoparticles are greatly dependent on the sizes of particles and surfaces of the species adsorbed. The readings obtained from the UV-Vis in the figure 3 below showed that the maximum wavelength of 420 nm, gave the highest absorbance for the silver nanoparticles synthesized through the reducing and stabilizing property of the chitosan. These nanoparticles exhibit a UV–Vis absorption maximum at the range of 400–500 nm due to their surface plasmon resonance.

Plate 1: Observing colour change in process of silver nanoparticles (AgNPs) formation with variation of time intervals starting from 0- 600 minutes (a) 0 minutes (b) 100 minutes (c) 300 minutes (d) 400 minutes (e) 500 minutes (f) 600 minutes.

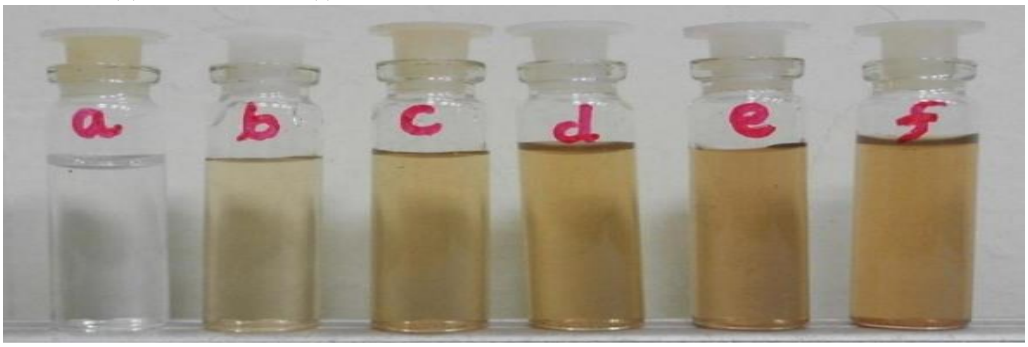

Figure 3: UV-Vis spectra recorded at various time intervals

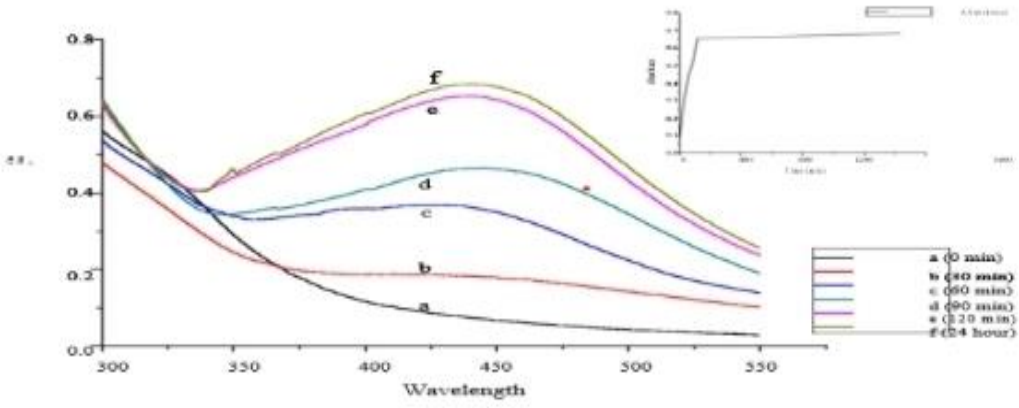

The reaction occurred rapidly as the formation of these nanoparticles took place steadily from 100 minutes with the increase in time showing a zero shift in wavelength peaks. After a period of 10 hours, there was no more rise in the absorption spectra due to the reason that each single ion had been consumed during the reduction phase. The UV-visible spectroscopic analysis confirmed the

Article DOI: https://doi.org/10.37284/ijpac.2.1.2242

presence of the synthesized silver nanoparticles (AgNPs) via the reduction method of silver ions in the solution when reacted with chitosan extracted from crab shells. They exhibited raw sienna coloured in the aqueous media due to surface plasmon resonance (SPR). The colour turned from clear to faint then yellow brown solution demonstrating the formation of the silver nanoparticles. These colour changes were consistent with the reported colour in the previous studies related to the extraction of silver nanoparticles. The plate 1 above shows the change in colour of silver nanoparticles synthesized with respect to change in time. The variation in coloration was brought about by visible light when refracted by the various sizes of nanoparticles formed in relation to the difference in time.

Results of absorbance at different levels of the synthesized silver nanoparticles using UV-Vis spectroscopy

Concentration of the silver nanoparticles samples was varied at three different levels starting from 1 mL Ag+, 10 mL Ag+ and 15 mL Ag+. On the other hand, the variations in chitosan concentration were conducted at 2.5, 5.0,10.0 and 15.0 pmm and applied to three different samples containing silver ions. The impact of increasing the concentration of chitosan solution on the three different levels of silver ions was monitored using UV-Vis spectroscopy as shown in figure 4 below. The results from the UV-Vis spectrophotometer showed an increasing trend in the absorbance as both solution's concentration was stepped up implying that absorbance is directly proportional to the concentration of the substance. The higher the concentration, the higher its absorbance. These observations were found to be consistent with the findings that chitosan acts both as a reducing and stabilizing agent. Therefore, an increase in the amount of silver ions and chitosan concentration elevated the reacting species in that system. The results obtained in the figure 4 (c) was therefore, considered most efficient in terms of time required for the formation of silver nanoparticles. From the data presented below, for quick synthesis of these nano-catalysts 20 ppm of chitosan with 15 mL Ag+ ions solution proved to be the most efficient and sufficient. Therefore, for the production of silver nanoparticles similar trend was also established in the previous studies done using chitosan as a reducing agent for the reaction (Osemba et al., 2024).

Figure 4 (a): UV-Visible spectral lines of Ag NPs formed at 1 mL Ag^+ ion conc. With variations in concentrations of chitosan a) 2.5 ppm b) 5 ppm c) 10 ppm. d) 15 pmm e) 20 ppm and f) 30 ppm

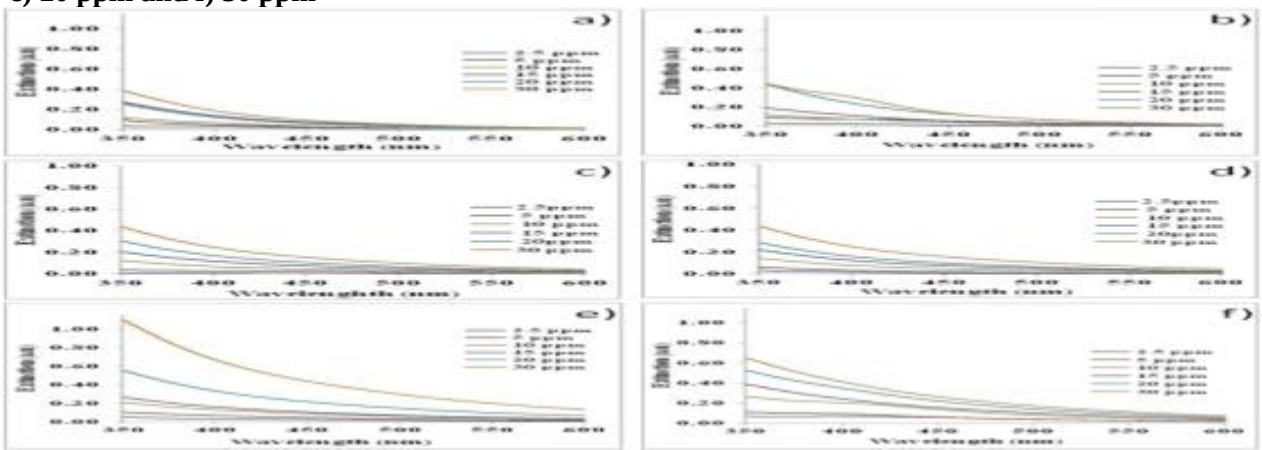

Article DOI: https://doi.org/10.37284/ijpac.2.1.2242

Figure 4 (b): UV-Visible spectral lines of Ag NPs formed at 10 mL Ag^+ ion conc. With variations in concentrations of chitosan a) 2.5 ppm b) 5 ppm c) 10 ppm. d) 15 pmm e) 20 ppm and f) 30 ppm

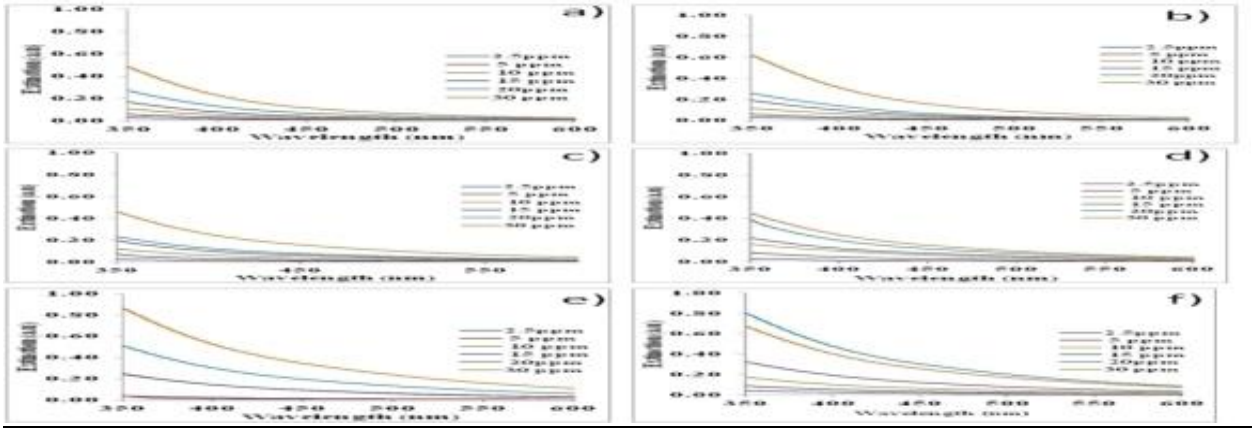

Figure 4 (c): UV-Visible spectral lines of Ag NPs formed at 15 mL Ag^+ ion conc. With variations in concentrations of chitosan a) 2.5 ppm b) 5 ppm c) 10 ppm. d) 15 pmm e) 20 ppm and f) 30 ppm

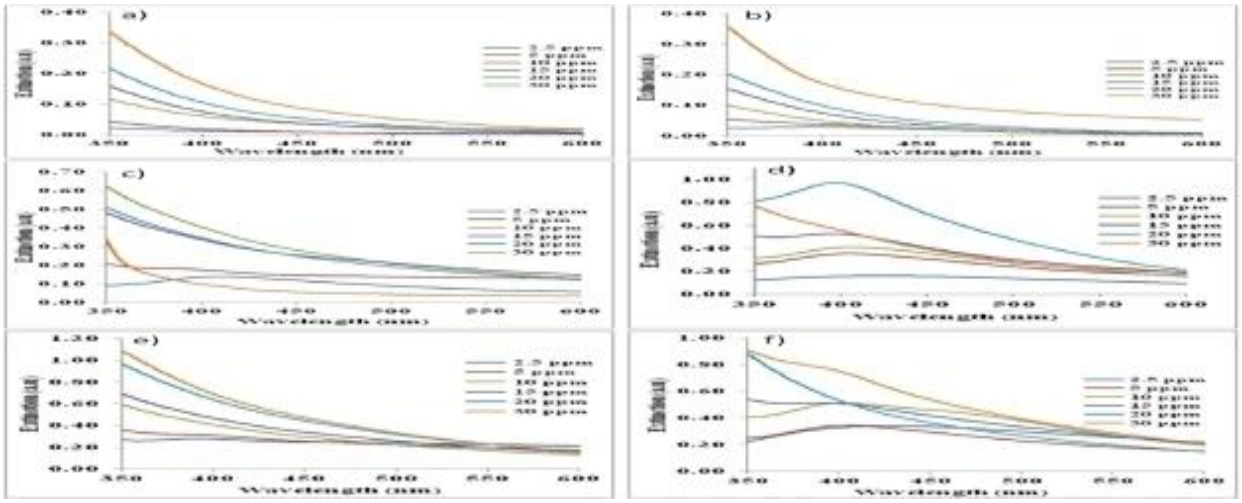

Scanning Electron Microscopy characterization of silver nanoparticles

Scanning microscope was used to validate the characterization of silver nanoparticles by giving nutshell description by providing the necessary information concerning the morphology of these silver nanoparticles. These images were taken at 500nm. The results of the nanoparticles as shown in the plates 2 *a, b, c* below show the results obtained from the scanning electron microscope (SEM) depicted a picture of these nanoparticles exhibiting size range of 100 nm which are in agreement with the earlier findings on the right sizes at different resolutions between 0.5 to 4 nm. Size of synthesized nanoparticles was more than the size of nanoparticles which should be between 1-100nm.

Article DOI: https://doi.org/10.37284/ijpac.2.1.2242

Plate 2 (a): Scanning electron microscope image of synthesized Silver Nanoparticles

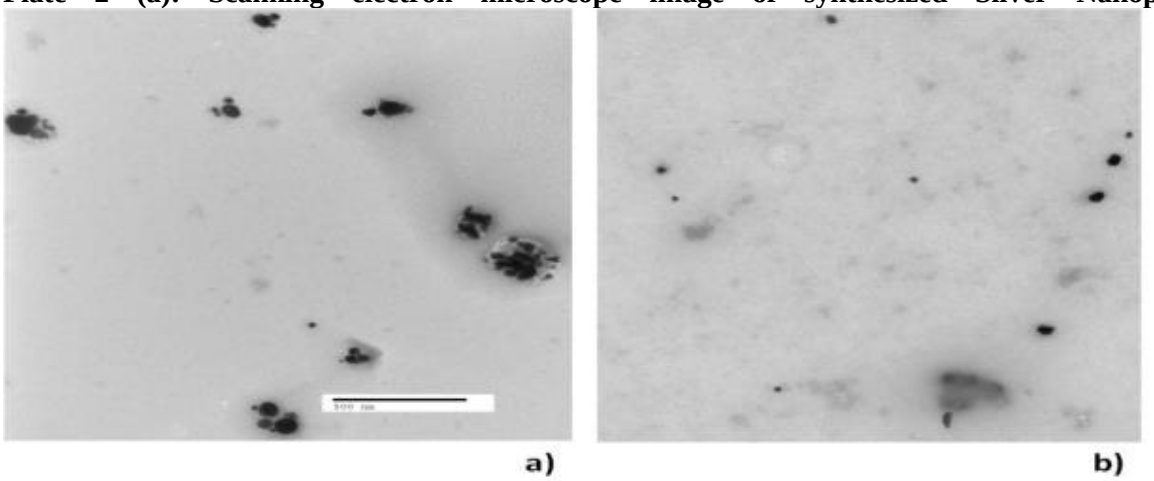

Plate 2 (b): Scanning electron microscope image of synthesized Silver Nanoparticles

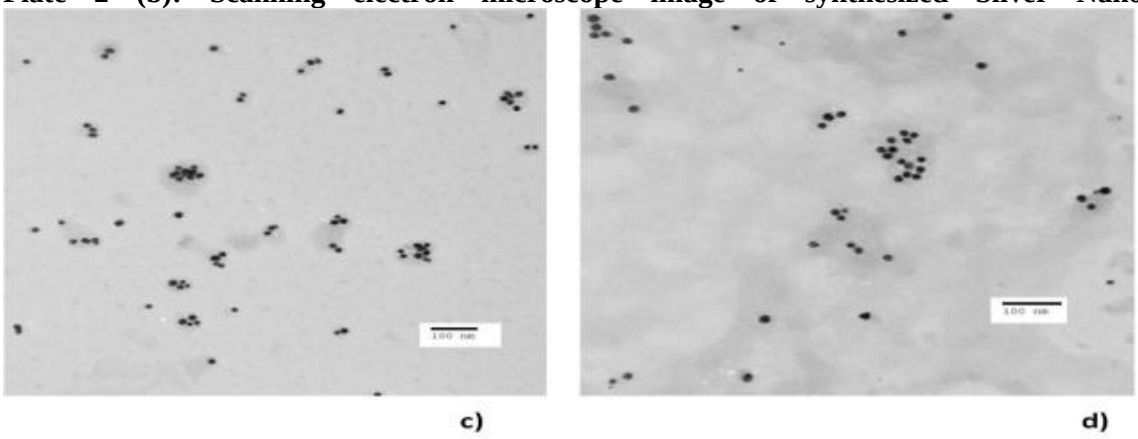

Plate 2 (c): Scanning electron microscope image of synthesized Silver Nanoparticles

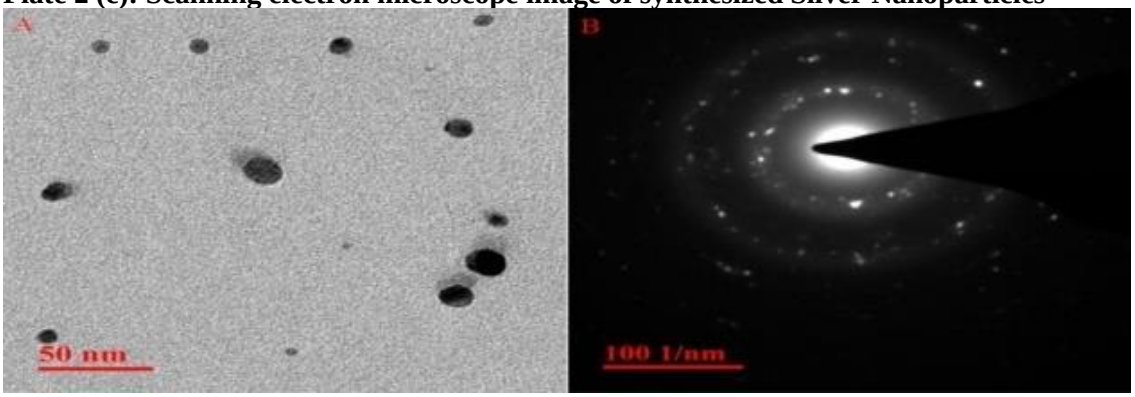

These results from SEM together with those from the UV-Vis studies give a clear affirmation of the presence of silver nanoparticles. This microscopic technique is directly applied in detecting and characterizing silver nanoparticles due to its ability to image these nanostructures, by directly determining their sizes, and furthermore, they present more information on the orientation of their shapes, even though they have limitation on the number of particles they can detect within a given time duration. This technique applies a high energy electron beam so that it undergoes scanning on

Article DOI: https://doi.org/10.37284/ijpac.2.1.2242

surface and back scattering of the electrons is in order to resonate. Therefore, the interaction between the atoms in the sample and high energy beam of electrons happen leading to the production of the signals providing details on the kind of surface topography, components present and the dialectical aspects of the nanoparticles. Initial size characterization of the silver nanoparticles synthesized using chitosan as a reducing method was done using UV-Vis spectrometry.

CONCLUSION

In conclusion, it was established that, the maximum absorbance from the UV-Vis of silver nanoparticles occurred at 418 nm. The FTIR analysis indicated a strong symmetrical stretching at 1400 cm^{-1} to 1200 cm^{-1} with the major peaks recorded at 1390 cm^{-1} and 1380 cm^{-1}, indicating the presence of nitro components in the sample. The signal at 1658 cm^{-1} corresponded to the amide (C=O) bonds stretching vibrations, at 1089 cm^{-1} C-O-C bonds and at 564 cm^{-1} plane with bends NH, plane-out and bends C−O. C-H stretching vibrational signal was noted at 2927 cm^{-1}, and a broader band at 3426 cm^{-1} with an overlap between the O−H stretching vibration and N−H stretching vibration of the oligosaccharide applied in the capping. The concentration of chitosan on transmittance was done using 0.5%, 1.0%, 1.5% and 2.0% solutions with the results from FT-IR showing elaborate intensity at 2.0 % chitosan capping and the least at 0.5 %. Scanning microscope validated characterized silver nanoparticles morphology at 500nm. The results obtained from SEM depicted a size range of 100 nm with resolutions between 0.5 to 4 nm.

REFERENCES

[1] Algethami, N., Rajeh, A., Ragab, H. M., Tarabiah, A. E., & Gami, F. (2022). Characterization, optical, and electrical properties of chitosan/polyacrylamide blend doped silver nanoparticles. *Journal of Materials Science: Materials in Electronics*, *33*(13), 10645–10656. https://doi.org/10.1007/s10854-022-08048-5

[2] Arshad, F., Naikoo, G. A., Hassan, I. U., Chava, S. R., El-Tanani, M., Aljabali, A. A., & Tambuwala, M. M. (2024). Bioinspired and Green Synthesis of Silver Nanoparticles for Medical Applications: A Green Perspective. *Applied Biochemistry and Biotechnology*, *196*(6), 3636– 3669. https://doi.org/10.1007/s12010-023-04719-z

[3] Ahmed, B., Tahir, M. B., Sagir, M., & Hassan, M. (2024). Bio-inspired sustainable synthesis of silver nanoparticles as next generation of nanoproduct in antimicrobial and catalytic applications. *Materials Science and Engineering: B*, *301*, 117165.

[4] Arshad, F., Naikoo, G. A., Hassan, I. U., Chava, S. R., El-Tanani, M., Aljabali, A. A., & Tambuwala, M. M. (2024). Bioinspired and Green Synthesis of Silver Nanoparticles for Medical Applications: A Green Perspective. *Applied Biochemistry and Biotechnology*, *196*(6), 3636– 3669. https://doi.org/10.1007/s12010-023-04719-z

[5] Azevedo, A. P. G., Müller, N., & Sant'Anna, C. (2024). Applications of silver nanoparticles in patent research. *Recent Patents on Nanotechnology*, *18*(3), 361–373.

[6] Behera, M., Behera, P. R., Sethi, G., Pradhan, B., Adarsh, V., Alkilayh, O. A., Samantaray, D. P., & Singh, L. (2024). Cyanobacterial Silver Nanoparticles and Their Potential Utility—Recent Progress and Prospects: A Review. *Journal of Basic Microbiology*, e2400256. https://doi.org/10.1002/jobm.202400256

[7] Bruna, T., Maldonado-Bravo, F., Jara, P., & Caro, N. (2021). Silver nanoparticles and their antibacterial applications. *International Journal of Molecular Sciences*, *22*(13), 7202.

Article DOI: https://doi.org/10.37284/ijpac.2.1.2242

[8] Choudhary, A., Singh, S., & Ravichandiran, V. (2022). Toxicity, preparation methods and applications of silver nanoparticles: An update. *Toxicology Mechanisms and Methods*, *32*(9), 650– 661. https://doi.org/10.1080/15376516.2022.2064257

[9] Dawadi, S., Katuwal, S., Gupta, A., Lamichhane, U., Thapa, R., Jaisi, S., Lamichhane, G., Bhattarai, D. P., & Parajuli, N. (2021). Current Research on Silver Nanoparticles: Synthesis, Characterization, and Applications. *Journal of Nanomaterials*, *2021*, 1–23. https://doi.org/10.1155/2021/6687290

[10] Fernandez, C. C., Sokolonski, A. R., Fonseca, M. S., Stanisic, D., Araújo, D. B., Azevedo, V., Portela, R. D., & Tasic, L. (2021). Applications of silver nanoparticles in dentistry: Advances and technological innovation. *International Journal of Molecular Sciences*, *22*(5), 2485.

[11] Husain, S., Nandi, A., Simnani, F. Z., Saha, U., Ghosh, A., Sinha, A., Sahay, A., Samal, S. K., Panda, P. K., & Verma, S. K. (2023). Emerging trends in advanced translational applications of silver nanoparticles: A progressing dawn of nanotechnology. *Journal of Functional Biomaterials*, *14*(1), 47.

[12] Kar, A., Giri, L., Almalki, W. H., Singh, S., Sahebkar, A., Kesharwani, P., & Dandela, R. (2024). Conclusion and future prospective of silver nanoparticles. In *Silver Nanoparticles for Drug Delivery* (pp. 433–452). Elsevier. https://www.sciencedirect.com/science/article/pii/B9780443153433000012

[13] Kaushal, A., Khurana, I., Yadav, P., Allawadhi, P., Banothu, A. K., Neeradi, D., Thalugula, S., Barani, P. J., Naik, R. R., & Navik, U. (2023). Advances in therapeutic applications of silver nanoparticles. *Chemico-Biological Interactions*, *382*, 110590.

[14] Kowalczyk, P., Szymczak, M., Maciejewska, M., Laskowski, Ł., Laskowska, M., Ostaszewski, R., Skiba, G., & Franiak-Pietryga, I. (2021). All that glitters is not silver—A new look at microbiological and medical applicatio ns of silver nanoparticles. *International Journal of Molecular Sciences*, *22*(2), 854.

[15] Naganthran, A., Verasoundarapandian, G., Khalid, F. E., Masarudin, M. J., Zulkharnain, A., Nawawi, N. M., Karim, M., Che Abdullah, C. A., & Ahmad, S. A. (2022). Synthesis, characterization and biomedical application of silver nanoparticles. *Materials*, *15*(2), 427.

[16] Nie, P., Zhao, Y., & Xu, H. (2023). Synthesis, applications, toxicity and toxicity mechanisms of silver nanoparticles: review. *Ecotoxicology and Environmental Safety*, *253*, 114636.

[17] . Osemba, M. O. (2019). *Electrochemical Degradation And Chemical Assessment Of Azo Dyes In The Textile Waste Water* [PhD Thesis, Pwani University]. https://elibrary.pu.ac.ke/handle/123456789/826

[18] Osemba, M. O., Muriuki-Hutchins, M., Karenga, S., & Keru, G. (2024). Production of Chitosan from Crab Shells. *International Journal of Advanced Research*, *7*(1), 244–250.

[19] Shehabeldine, A. M., Salem, S. S., Ali, O. M., Abd-Elsalam, K. A., Elkady, F. M., & Hashem, A. H. (2022). Multifunctional silver nanoparticles based on chitosan: Antibacterial, antibiofilm, antifungal, antioxidant, and wound-healing activities. *Journal of Fungi*, *8*(6), 612.

[20] Younis, M. A. (2024). Clinical translation of silver nanoparticles into the market. In *Silver Nanoparticles for Drug Delivery* (pp. 395–432). Elsevier. https://www.sciencedirect.com/science/article/pii/B9780443153433000073

